

# Thermomechanical properties of alumina fiber membrane

J.A. Fernando<sup>1</sup>, D.D.L. Chung\*

*Composite Materials Research Laboratory, University at Buffalo,  
The State University of New York, Buffalo, NY 14260-4400, USA*

Received 28 February 2004; received in revised form 23 May 2004; accepted 15 June 2004

Available online 1 September 2004

## Abstract

The use of an acid phosphate binder in place of a commercial silica colloid binder in the fabrication of an alumina fiber membrane was found to result in improved creep resistance (as tested under compression at 600 and 800 °C), increased flexural strength (as tested up to 800 °C), increased storage modulus and damping capacity (as tested up to 500 °C), and decreased thermal conductivity (as tested at 600 and 800 °C), in addition to the previously reported increased permeability and compressive strength at room temperature.

© 2004 Elsevier Ltd and Techna Group S.r.l. All rights reserved.

**Keywords:** B. Fiber; C. Creep; C. Strength; C. Thermal conductivity; D. Alumina; Ceramic membrane

## 1. Introduction

Porous ceramic membranes with pore size ranging from 0.1 to 50 µm and porosity above about 40% are used for filtration (e.g., hot gas filtration), diffusion (e.g., waste water treatment), dispersion rolls, ink pads for fingerprinting and numerous other applications. In particular, filtration is important for the petrochemical, mining and chemical industries.

Ceramic membranes can be made from particles or discontinuous fibers by the use of a binder or by sintering. Due to the high temperature required by sintering, the binder route is much more cost effective. Binders are most commonly in the form of a fine particle dispersion (colloid). The silica colloid is an example. After application by wet forming (as in paper making), drying and appropriate heat treatment are needed.

The binder technology is central to the technology of membrane fabrication. A binder is necessary to hold the

ceramic particles or fibers together to form a membrane. It must be used in a sufficient quantity in order for the membrane to have acceptable mechanical strength. However, it must not block the pores in the membrane, as is the case if it is used excessively. Thus, an effective binder should be able to bind the particles or fibers together and result in a mechanically strong membrane, even when it is used in a very small proportion. In addition, the binder must be able to withstand high temperatures, as encountered in hot gas filtration.

Silica and vitreous glass are widely used binders in the refractory and ceramic industry [1]. It is often used in the form of an aqueous dispersion. The silica colloid is particularly attractive due to the high temperature resistance of silica compared to vitreous glass and the good binder dispersion enabled by the small particle size of the silica in the colloid. The average size of the silica particles in the colloid can range from under 10 nm to over 80 nm. The silica binder is easy to use, but it tends to fill the open or continuous porosity of the filter membrane.

Phosphate has been utilized as a binder in the refractory industry for many years [2–4]. Pirogov et al. [5] used a phosphoric acid (H<sub>3</sub>PO<sub>4</sub>) binder in a mullite-corundum body in their study to determine the optimum content of graphite and SiC additives. Birchall et al. [6] studied the mechanical

\* Corresponding author. Tel.: +1 716 645 2593x2243;

fax: +1 716 645 3875.

E-mail address: jfernando@unifrax.com (J.A. Fernando),  
ddlchung@buffalo.edu (D.D.L. Chung).

<sup>1</sup> Permanent address: Unifrax Corporation, Corporate Headquarters,  
2351 Whirlpool Street, Niagara Falls, NY 14305-2413, USA.

properties of an unsintered SiC compact bonded by aluminum phosphate ( $\text{AlPO}_4$ ) glass. Toy and Whitemore [7] evaluated the reactivities of several calcined aluminas with phosphoric acid and demonstrated that a glassy  $\text{AlPO}_4$  phase and aluminum metaphosphate ( $\text{Al}(\text{PO}_3)_3$ ) are effective bonding phases. Phosphoric acid has also been shown to be effective for bonding refractory castables composed of sintered aluminum oxide [8]. These castables are characterized by high bond strength and high resistance to erosion over a wide temperature range. Monoaluminum phosphate ( $\text{Al}(\text{H}_2\text{PO}_4)_3$ ) and magnesium phosphate ( $\text{Mg}(\text{H}_2\text{PO}_4)_2$ ) are also reported to be suitable for use in refractory and ceramic foam applications [1].

Gitzen et al. [8] outlined three methods of using phosphate bonding in refractory materials: (1) the use of siliceous materials with phosphoric acid, (2) the use of oxides with phosphoric acid, and (3) the direct addition or formation of an acid phosphate. The addition of aluminum significantly increases the bonding capability of acid phosphates [2–4].

Chiou and Chung [1] developed aluminum phosphate binders (in solution form rather than colloidal form, thus allowing effectiveness at even a small binder proportion) with various P/Al molar ratios and demonstrated that a P/Al ratio of 23 (binder designation of A23) resulted in the highest bonding strength when used with SiC whiskers and short carbon fibers. The aluminum phosphate binders developed by Chiou and Chung were called acid phosphates because they contained phosphoric acid in excess of what is needed to form aluminum phosphate.

X-ray diffraction [1] showed that, when the A23 binder (by itself) was heat treated at 200 °C, it remained in an amorphous form. Crystallization was shown to occur after heat treating the A23 binder to 500 or 800 °C to form mainly type-A aluminum metaphosphate  $\text{Al}(\text{PO}_3)_3$ . After heat treating at 1100 °C in air, the A23 binder became amorphous again. The amorphous phase was thought to be a metaphosphate glass [1]. After heating the binder at 1200 °C in argon, the A23 binder was mainly amorphous, although a minor amount of a crystalline phase was also present. The minor crystalline phase was thought to be the cristobalite aluminum orthophosphate  $\text{AlPO}_4$  [1].

This paper addresses a ceramic membrane that has been improved by using a low-cost binder in the form of an acid phosphate. The binder is made by dissolving aluminum hydroxide in phosphoric acid to form a liquid solution. The composition is described in the following: P/Al = 23; P from phosphoric acid (in excess of what is needed to form aluminum phosphate); Al from aluminum hydroxide; low-cost ingredients; solution form (not colloidal form); Type-A  $\text{Al}(\text{PO}_3)_3$  after heating; and 9–10 wt.% in the case of a fiber membrane. The acid phosphate binder can be used to make a ceramic membrane by incorporating it in a water-based dispersion containing the ceramic particles or fibers and subjecting the dispersion to wet forming, followed by heat treatment.

Properties of the alumina fiber membranes made using commercially available binders were compared [9] to membranes made using the A23 acid phosphate binder [11]. This patent [11] covers the binder material, although it is not directed at use of the binder in making a membrane, but use of the binder in making a porous particulate or fibrous preform for making metal-matrix composites by liquid metal infiltration. The alumina filter membrane containing the acid phosphate binder exhibits the highest flexural strength, compressive strength, work of fracture and elastic modulus in comparison to those containing the other binders (silica, alumina and monoaluminum phosphate) at equivalent binder contents [9].

Microscopy showed that the acid phosphate binder causes the fibers to bond at their junctions only [9], whereas the colloidal silica binder causes free binder particles within the fiber network. The membranes containing acid phosphate exhibits the lowest pressure drop in comparison to membranes with other binders having equivalent flexural and compressive strengths [9]. The pore size distribution is narrow in comparison to silica-bonded membranes [10]. The filter membrane containing the acid phosphate binder has a mean flow pore size of  $2.6 \pm 0.1 \mu\text{m}$ , whereas the silica-bonded filter membrane has a mean flow pore size of  $4.8 \pm 0.1 \mu\text{m}$  [10]. The permeability of the acid phosphate-bonded membrane is approximately four times that of the silica-bonded membrane [10].

In contrast to prior work [9,10], this paper is focused on the thermomechanical behavior, which is important to hot gas filtration and related applications. The superiority of the alumina fiber membrane made with the acid phosphate binder over that made with the silica binder pertains to (i) higher flexural strength (tested up to 800 °C) ([9], this work), (ii) higher compressive strength [9], (iii) higher work of fracture [9], (iv) higher elastic modulus (tested up to 500 °C) ([9], this work), (v) better creep resistance (tested up to 800 °C) (this work), (vi) higher damping capacity (tested up to 500 °C) [this work], (vii) higher air permeability [10], and (viii) narrower pore size distribution [10].

## 2. Experimental methods

Thermal and thermomechanical properties were evaluated in this work for acid phosphate and silica (Ludox HS40, DuPont, Wilmington, DE; 12  $\mu\text{m}$  particle size, 220  $\text{m}^2/\text{g}$  specific surface area, 40 wt.% solids content) bonded alumina fiber based filter membranes. The ingredients, processing, composition and other properties of these membranes are as described in Section 1 and Ref. [9].

The alumina fiber (Saffil, ICI Performance Chemicals, Cheshire, UK; RF milled, 3  $\mu\text{m}$  mean diameter, 115  $\mu\text{m}$  mean length, 3.3  $\text{g}/\text{cm}^3$  density, 1–2 GPa tensile strength,  $\delta$ -alumina) was the same as that used in Ref. [9]. As in Ref. [9], alumina fiber membranes were made by wet forming (with 1 part of binder to 15 parts of water, and filtration of the slurry

through a 200 mesh stainless steel screen) and heat treatment (placing in a pre-heated 300 °C furnace, increasing the temperature to 800 °C at a rate of 20 °C/min and then holding at 800 °C for 3 h), with pressure (10.5 or 17.5 kPa) optionally applied during wet forming to control the density.

The high temperature creep properties of the alumina fiber membrane were studied at a constant compressive stress. A vertically mounted tube furnace was used in combination with an MTS hydraulic mechanical testing system to record the strain versus time at temperatures of 400, 600 and 800 °C for 500 min. A constant compressive stress of 0.4 MPa was applied to all specimens during testing. For comparison, the compressive yield stresses for the silica and acid phosphate-bonded filter membranes are approximately 0.8 and 1.1 MPa, respectively.

The high temperature flexural strength of the alumina fiber membrane was measured using a three-point loading fixture that was placed in a vertically mounted tube furnace (similar to the apparatus used for creep testing). An MTS hydraulic mechanical testing system was used to determine the flexural strength at 400, 600 and 800 °C. Five specimens of each type were tested at each temperature. The work of fracture was determined by dividing the area under the load versus displacement curve by the fracture surface area, which is twice the projected area of one fracture surface.

Dynamic mechanical properties [18] were measured using the DMA 7e dynamic mechanical analyzer (Perkin-Elmer Corp., Norwalk, CT, USA). The system included an analyzer, a furnace with temperature program control, a computer and a measuring system. The measuring system consisted of a force motor which applied a sinusoidal force to the specimen, a displacement transducer (LVDT) which measured the response of the specimen, and a probe which transmitted the force from the motor to the specimen. The specimen was mounted on a bending platform in a three-point bending mode. During operation, the force motor provided a sinusoidal time-varying force to the specimen.

Dynamic mechanical testing (ASTMD 4065-94) at controlled frequencies (0.20, 1.00 and 5.00 Hz) was conducted under three-point flexure as a function of temperature (from room temperature to 500 °C) using the dynamic mechanical analyzer in the temperature scan mode. The heating rate was 5 °C/min, which was selected to prevent any artificial damping peaks that may be caused by higher heating rates. The specimens were in the form of beams (3 mm × 8 mm × 25 mm) under three-point bending, such that the loading span was 20 mm. The loads used were all large enough so that the amplitude of the specimen deflection was always over the minimum value of 5 µm, required by the equipment for accurate results. The loads were set so that each different type of specimen was always tested at its appropriate stress level. Six specimens of each density were tested.

The thermal conductivity (in W/m K) is given by the product of the thermal diffusivity (in mm<sup>2</sup>/s), specific heat (in J/g K) and density (in g/cm<sup>3</sup>) [20]. The thermal diffusivity was measured using a Flashline 3000 Thermal

Diffusivity System, made by Anter Corporation, Pittsburgh, PA. The flash method used a high speed xenon discharge pulse source directed to the top face of the specimen to increase the temperature of the specimen by  $\Delta T$  as a function of time.

The specimens used for thermal diffusivity testing were in the form of a disc, with a diameter of 25 mm and a thickness of 3 mm. Specimen preparation involved (1) ensuring surfaces were smooth and flat using a 400 grit SiC grinding paper, and (2) coating both sides of the sample with carbon for thermal contacts and to avoid reflection of the xenon discharge light beam. Three specimens were tested at each of three temperatures (600, 800 and 1000 °C).

A differential scanning calorimeter (model STA-449-C, made by Netzsch, Raleigh, North Carolina) was used for measuring the specific heat. A three-curve analysis method was used; it involved obtaining a specimen, baseline, and reference materials data. Sapphire was used as the reference material. Three specimens of each type were tested.

The coefficient of thermal expansion was measured using a push rod dilatometer (Model Unitherm 1091-SX140) made by Anter Corporation, Pittsburgh, PA, USA. The dilatometer used a fused silica tube and push rod. The thermal expansion tests were performed according to the specifications of ASTM E228 Test Method. The specimen size was 6 mm × 6 mm × 25 mm. The expansion measurements were taken using the 25 mm specimen dimension as the starting point. Three specimens were tested up to 1000 °C and heated at a rate of 2 °C/min.

### 3. Results and discussion

#### 3.1. Creep

Fig. 1 shows the compressive strain of the specimens tested at 400 °C. Within experimental error, no difference is seen between the acid phosphate-bonded alumina fiber filter membrane material (density = 0.285 g/cm<sup>3</sup>) and the silica-bonded specimen (density = 0.285 g/cm<sup>3</sup>). The specimens

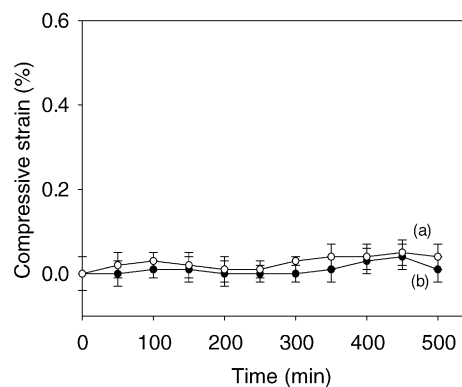


Fig. 1. Creep performance of alumina fiber membranes at 400 °C under a constant stress of 400 kPa: (a) acid phosphate binder and (b) silica binder.

tested at 600 °C (Fig. 2) shows that the silica-bonded alumina fiber membrane material exhibits increasing compressive strain beginning at around 100 min. At 500 min, the silica-bonded sample shows approximately 0.14% compressive strain, in comparison to 0.04% strain exhibited by the acid phosphate-bonded material.

Fig. 3 compares the creep behavior of the silica-bonded and acid phosphate-bonded specimens tested at 800 °C. The difference in creep performance between the two binders is significant. The acid phosphate-bonded material shows a small amount of compressive creep at 0.04%. In comparison, the silica-bonded specimen shows a compressive creep strain of 0.5%.

The good creep performance of the acid phosphate-bonded alumina fiber filter material is consistent with the high temperature storage modulus (Section 3.3) and the crystallization of the aluminum phosphate [9]. The good creep properties of phosphate-bonded ceramic materials is consistent with work reported by Martin and Talmy [12], who studied the creep rates of phosphate-bonded  $\text{Si}_3\text{N}_4$ , AlN and  $\text{Al}_2\text{O}_3$  powders. Their work compared the bonding properties of aluminum phosphate ( $\text{AlPO}_4$ ), zirconium phosphate ( $\text{ZrP}_2\text{O}_7$ ) and silicon phosphate ( $\text{Si}_3(\text{PO}_4)_4$ ) in creep performance and other high temperature mechanical properties. Their work also showed that  $\text{Si}_3\text{N}_4$  powder bonded with silicon phosphate and  $\text{Al}_2\text{O}_3$  powder bonded with aluminum phosphate exhibited the highest strength and the material made with the aluminum phosphate binder used in combination with AlN powder exhibited a much higher creep resistance in comparison to the  $\text{Si}_3\text{N}_4$  based materials using whatever binder. The lower creep resistance of the  $\text{Si}_3\text{N}_4$ -based materials at a high temperature (800 °C) was attributed the formation of silicon phosphate which melted at 1100 °C.

The relative creep deformation that develops in a given material exposed to a load depends on the load intensity and duration, exposure temperature of the load and material parameters (grain size, porosity, phase distribution and crystal structure) [13]. It has been reported by Jokačević et al. [14] that the behavior of a refractory material exposed to a high temperature and a high load is influenced significantly

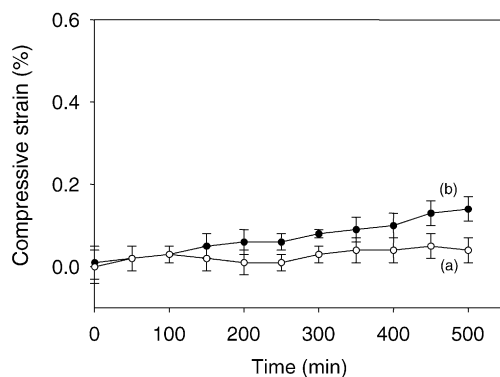


Fig. 2. Creep performance of alumina fiber membranes at 600 °C under a constant stress of 0.4 MPa: (a) acid phosphate binder and (b) silica binder.

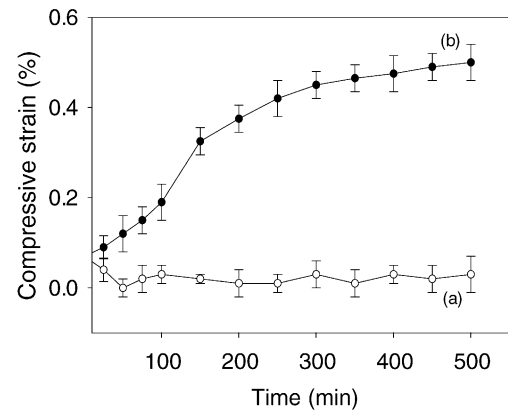


Fig. 3. Creep performance of alumina fiber membranes at 800 °C under a constant stress of 0.4 MPa: (a) acid phosphate binder and (b) silica binder.

by the presence of a glassy phase. Jokačević et al. [14] showed that the degrading effect of the presence of a glassy phase is evident when the glassy phase is concentrated along the grain boundaries in a refractory ceramic material. The glassy phase, if allowed to penetrate into the grain boundaries, will degrade the ceramic material by weakening the intergranular bonds. This situation, although applicable to higher density refractory ceramic materials, is analogous to the alumina fiber based filter membrane made using the colloidal silica binder. At an elevated temperature and under a constant load, creep deformation will occur in alumina fiber membranes when silica is used. The creep deformation in this system is attributed to the viscous flow of the glassy silica binder material [14].

In porous alumina materials fabricated by sintering (without a binder), the creep properties are superior in comparison to porous ceramic materials using a binder phase. For example, in alumina fiber based porous ceramic materials that use a silica binder as part of the fabrication process, the binder material is the main source of creep. Although the sintering fabrication approach will result in superior creep resistance, the high cost associated with this method makes it unattractive in comparison to processes that use binders.

Although the importance of creep resistance is recognized by others involved in the development and testing of high temperature filter membranes [15], relatively little work has been done previously to improve the creep resistance by using improved binders.

### 3.2. High temperature flexural strength

Fig. 4 shows the results of the flexural strength measurements made at 400, 600 and 800 °C. For comparison, the room temperature measurements have also been plotted on the same graph.

The results indicate that the acid phosphate binder gives better flexural strength not only at room temperature but also at elevated temperatures in comparison to the silica binder

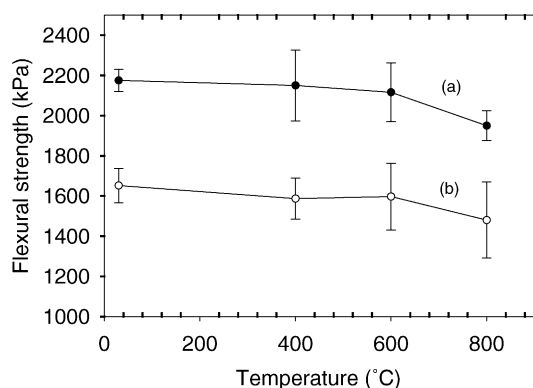


Fig. 4. Graph showing flexural strength measured as a function of temperature for an alumina fiber membrane made using (a) acid phosphate binder and (b) silica binder.

used at the same level. Above 600 °C there is a noticeable reduction in strength for both acid phosphate and silica binders. The reduction in the strength above 600 °C in the silica-bonded filter membrane is attributed to the glassy silica binder phase that undergoes viscous flow deformation resulting from the applied stress at the elevated temperature [24]. In the case of the specimen with the acid phosphate binder, X-ray diffraction shows that, after exposure to the fabrication temperature of 800 °C, the binder phase is primarily crystalline [9]. However, based on the present elevated temperature flexural strength results and the results from other studies [13,16,17], it is proposed that a minor amorphous phase is present and undergoes softening, thereby allowing the bonded fiber junctions to lose some strength.

The work of fracture (Fig. 5) does not decrease when tested at 800 °C. Even though the strength is lower (Fig. 4), the area under the curve of load versus displacement remains approximately the same because of energy absorption during the more gradual failure of the membrane due to the softened binder medium.

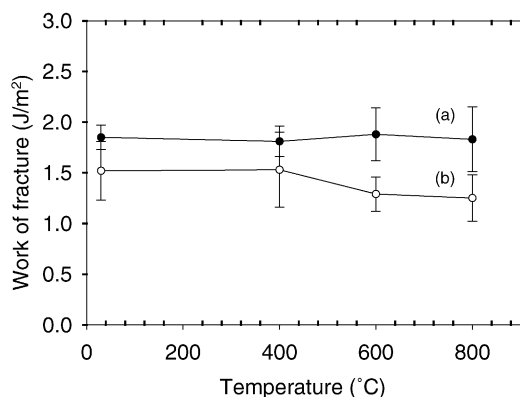


Fig. 5. Graph showing the work of fracture, measured as a function of temperature, for an alumina fiber membrane made using (a) acid phosphate binder and (b) silica binder.

### 3.3. Dynamic storage modulus and damping capacity

Fig. 6 shows the variation of the dynamic storage modulus with increasing temperature for the alumina fiber membrane with the acid phosphate binder. The results show an increase in the storage modulus with increasing frequency as well as an increase in storage modulus with increasing temperature above 300 °C. In comparison, the silica-bonded alumina fiber membrane shows little change with increasing frequency or increasing temperature (Fig. 7). The reason for the significant variation of the dynamic storage modulus with frequency in the case of the acid phosphate binder is unclear. A more detailed analysis of this phenomena is necessary to understand the relationship between frequency and dynamic modulus.

Increase in the dynamic storage modulus with increasing temperature was reported by Chia et al. [18] in their work to determine the mechanical properties of  $\text{ZrO}_2/\text{NiCoCrAlY}$  composite coatings. The reason for the increase in storage modulus with increasing temperature in their system was ascribed to mechanisms related to crystalline phase changes with increasing temperature and the different dynamic mechanical properties of the crystalline phases. Similarly, the increase in storage modulus with increasing temperature in the acid phosphate-bonded alumina fiber membrane (Fig. 6) is attributed to the crystallization taking place in the aluminum phosphate system. It was demonstrated in our earlier work [9] that, between the 400 and 600 °C heat treatment stages, the aluminum phosphate system transforms from a primarily amorphous phase to a system having crystalline phases of berlinite  $\text{AlPO}_4$  and type-A  $\text{Al}(\text{PO}_3)_3$ . The temperature range in which this crystallization occurs corresponds to the temperature range in which an increase in storage modulus is observed.

Similarly, the lack of any change in storage modulus with increasing temperature or frequency in the case of the silica-bonded alumina fiber membrane is consistent with the fact that silica remains amorphous in the temperature range of

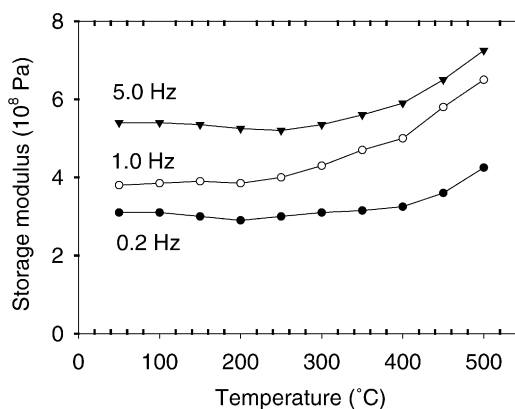


Fig. 6. Storage modulus of alumina fiber membrane made with the acid phosphate binder plotted as a function of temperature.



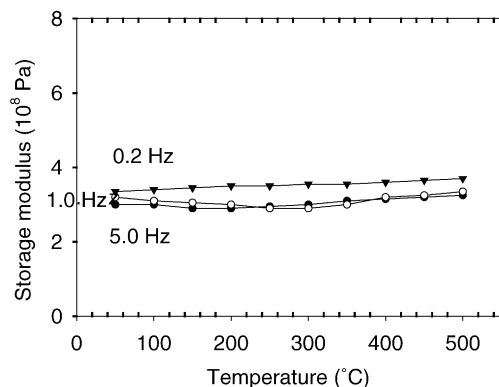


Fig. 7. Storage modulus of alumina fiber membrane made with the silica binder plotted as a function of temperature.

the test. In comparing the results of the acid phosphate-bonded membrane with those of the silica-bonded membrane (Figs. 6 and 7), it is evident that the acid phosphate-bonded membrane, at temperatures below 300  $^{\circ}$ C and at 0.2 Hz, has a storage modulus that is approximately the same as that of the silica-bonded membrane. At higher temperatures (above 300  $^{\circ}$ C) and at higher frequencies (1.0 and 5.0 Hz), the acid phosphate-bonded membrane has a higher dynamic storage modulus.

In the case of the acid phosphate-bonded alumina fiber membrane, it is expected that, if the storage modulus is measured for temperatures higher than 500  $^{\circ}$ C, the storage modulus will increase up to a certain critical temperature above 500  $^{\circ}$ C due to increased crystallization and then begin to decrease with further increase in temperature due to the formation of cristobalite  $\text{AlPO}_4$  and eventually an amorphous phase. The experiments conducted in the present study were not done above 500  $^{\circ}$ C due to limitations of the test equipment.

Fig. 8 shows the variation in the damping capacity (a measure of a material's ability to dissipate elastic strain energy during mechanical vibration or wave propagation),  $\tan \delta$ , with increasing temperature for the alumina fiber membrane with the acid phosphate binder. Little difference is seen for the results tested at the three frequencies, namely,

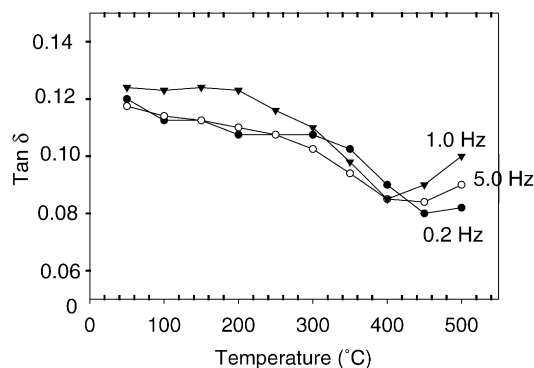


Fig. 8. Damping capacity ( $\tan \delta$ ) of alumina fiber membrane made with the acid phosphate binder plotted as a function of temperature.

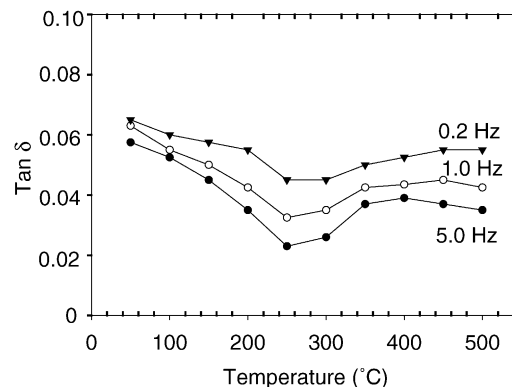


Fig. 9. Damping capacity of alumina fiber membrane made with the silica binder plotted as a function of temperature.

0.2, 1.0 and 5.0 Hz. All three curves indicate a drop in damping capacity with increasing temperature, although at around 400  $^{\circ}$ C all the specimens begin to show an increase in damping capacity. In comparison, the alumina fiber membrane made with the silica binder (Fig. 9) exhibits lower values of the damping capacity.

A reduction in damping capacity implies a reduction in the energy dissipated by the specimen. Among the various damping mechanisms, internal friction makes a large contribution to the overall damping in dense crystalline materials [19]. Therefore, a reduction in the energy dissipated by the present alumina fiber based porous specimen is possibly due to a reduction in internal friction caused by the same mechanisms that increase the dynamic storage modulus. A more comprehensive analysis of the dynamic storage modulus properties and damping capacity is required to identify the active mechanisms in the present alumina fiber based filter membrane under dynamic loading conditions. An in-depth evaluation of the dynamic material characteristics, mechanisms of deformation and energy storage/dissipation and the effects of different process variables would require further detailed analysis that is beyond the scope of the present work. Nevertheless, it is technologically significant that the acid phosphate binder gave higher storage modulus as well as higher damping capacity than the silica binder.

### 3.4. Thermal conductivity

The thermal diffusivity, specific heat, and density were measured for acid phosphate-bonded membranes of densities 0.255 and 0.315  $\text{g/cm}^3$  and a silica-bonded membrane of density 0.318  $\text{g/cm}^3$ . For each membrane, three temperatures, namely 600, 800 and 1000  $^{\circ}$ C, were used. Table 1 shows these values and the thermal conductivity values that were calculated for each of these membranes.

To illustrate the effect of density on thermal conductivity of the alumina fiber filter membranes using acid phosphate binder, Fig. 10 shows the thermal conductivity values for the two acid phosphate-bonded membranes plotted as a function of temperature. The lower density material at 600  $^{\circ}$ C has

Table 1

Thermal diffusivity, specific heat, density at temperature and thermal conductivity of alumina fiber filter membrane materials

Specimen type	Temperature (°C)	Thermal diffusivity (mm <sup>2</sup> /s)	Specific heat (J/g K)	Density at temperature (g/cm <sup>3</sup> )	Thermal conductivity (W/m K)
1	600	0.60	1.20	0.22	0.16
	800	0.65	1.28	0.22	0.18
	1000	0.70	1.36	0.22	0.21
2	600	0.28	1.20	0.29	0.10
	800	0.35	1.28	0.29	0.13
	1000	0.43	1.36	0.29	0.17
3	600	0.42	1.19	0.32	0.16
	800	0.47	1.27	0.32	0.18
	1000	0.48	1.35	0.32	0.19

(1) Acid phosphate-bonded membrane of density 0.255 g/cm<sup>3</sup>, (2) acid phosphate-bonded membrane of density 0.285 g/cm<sup>3</sup>, (3) silica-bonded membrane of density 0.285 g/cm<sup>3</sup>.

about 61% higher thermal conductivity in comparison to the higher density specimen. At 1000 °C, the thermal conductivity of the lower density material is about 22% higher than that of the higher density material. The increase in density and the corresponding improvement in the ability of a fibrous ceramic material to be thermally insulating is consistent with work reported by others [21]. It has been reported for fibrous ceramic materials that increasing density up to about 0.4 g/cm<sup>3</sup> will decrease the thermal conductivity because air is more effectively trapped and radiation is blocked more completely [21]. At densities beyond about 0.4 g/cm<sup>3</sup>, heat transfer via conduction through the solid medium begins to contribute more and the thermal conductivity begins to increase with increasing density.

In comparing the thermal conductivity of the silica-bonded membrane to that of the acid phosphate-bonded membrane, both of density around 0.315 g/cm<sup>3</sup>, Fig. 11 shows that the silica-bonded membrane exhibits a higher thermal conductivity (especially at 600 and 800 °C). The fiber type, the bulk density and the amount of binder are the same for both membranes; the only difference is in the type of binder. The silica-bonded alumina fiber membrane has silica particles lodged within the fiber network and the fibers in this membrane are often ‘bundled’ together [9]. It is

suggested that a possible reason for the higher thermal conductivity in the silica-bonded filter membrane is due to an increased contribution of heat transfer by conduction through the solid material. Silica particles that are not at the junctions of fibers or bundled fibers will increase the ‘contact points’ for a given volume of the porous ceramic material, thereby increasing the heat transfer by conduction.

The relatively low thermal conductivity of the membrane made with the acid phosphate binder is attractive for hot gas filtration, because thermal losses to the steel structure and temperature losses in the gas stream can be reduced.

### 3.5. Thermal expansion

The average thermal expansion coefficients of acid phosphate-bonded membranes (densities 0.255 and 0.285 g/cm<sup>3</sup>) at 25–1000 °C is  $7.3 \times 10^{-6}/^{\circ}\text{C}$ . In comparison, the silica-bonded membrane (density 0.285 g/cm<sup>3</sup>) has an average thermal expansion coefficient of  $6.9 \times 10^{-6}/^{\circ}\text{C}$ . The slightly lower thermal expansion coefficient of the silica-bonded membrane is not interpreted as being significant enough to make a difference in an application such as a hot gas filtration. No abrupt change in slope due to phase transformation is observed in any of the membranes at these temperatures.

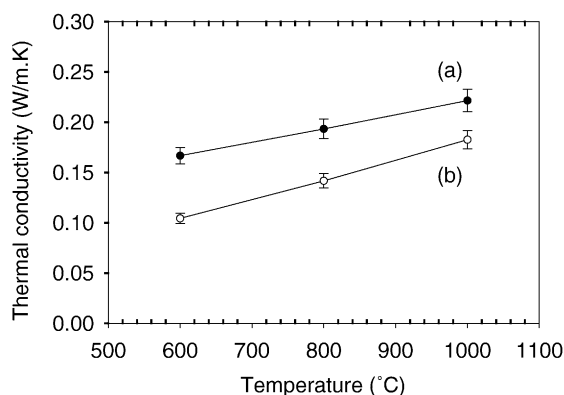


Fig. 10. Comparison of the thermal conductivity of the acid phosphate-bonded alumina fiber membranes at densities of (a) 0.255 g/cm<sup>3</sup> and (b) 0.315 g/cm<sup>3</sup>.

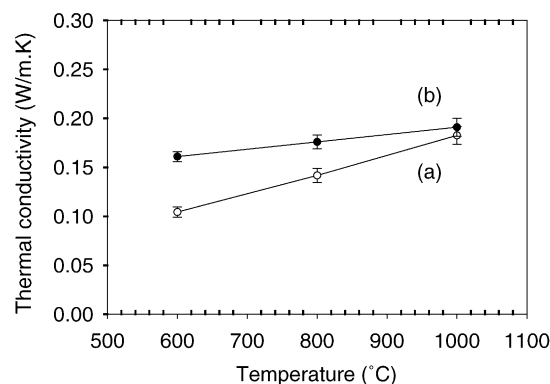


Fig. 11. Comparison of the thermal conductivity of alumina fiber membranes made by using (a) the acid phosphate binder at a density of 0.315 g/cm<sup>3</sup> and (b) the silica binder at a density of 0.318 g/cm<sup>3</sup>.

The results from the thermal expansion experiments are also used in Section 3.4 to calculate the density when the material is at a high temperature, so that a more accurate thermal conductivity value can be calculated.

#### 4. Conclusion

Alumina fiber membrane made by using the acid phosphate binder is superior to that made by using the silica binder in the creep resistance, high temperature flexural strength, storage modulus and damping capacity. In addition, the former is advantageous in its lower thermal conductivity and in the previously reported higher permeability and compressive strength.

Within experimental error, no difference is seen between the acid phosphate-bonded alumina fiber membrane and the silica-bonded membrane when creep tested at 400 °C. However, when creep tested at 600 °C, the silica-bonded membrane exhibits 0.14% compressive strain in comparison to 0.04% strain demonstrated by the acid phosphate-bonded material. The significant difference in creep performance between the two binders becomes even clearer when tested at 800 °C. The acid phosphate-bonded membrane shows a relatively small amount of compressive creep at 0.04%. In comparison, the silica-bonded membrane shows a much higher compressive creep strain of 0.5%.

The acid phosphate binder gives better flexural strength not only at room temperature but also at temperatures up to 800 °C in comparison to the silica binder used at the same level.

Comparison of the thermal conductivity of the silica-bonded membrane to that of the acid phosphate membrane of equivalent density indicates that the silica-bonded membrane exhibits a higher thermal conductivity, particularly at 600 and 800 °C.

The acid phosphate-bonded alumina fiber membrane exhibits higher storage modulus as well as higher damping capacity in comparison to the silica-bonded membrane. The former also shows an increase in the dynamic storage modulus with increasing frequency and with increasing temperature above 300 °C. In comparison, the latter shows little change in the dynamic storage modulus with increasing frequency or temperature. The increase in dynamic storage modulus with increasing temperature in the acid phosphate-bonded membrane is attributed to crystallization in the aluminum phosphate system.

The coefficient of thermal expansion is essentially the same for acid phosphate-bonded and silica-bonded membranes. The value is  $7 \times 10^{-6}/^{\circ}\text{C}$ .

#### References

- [1] J.M. Chiou, D.D.L. Chung, Improvement of the temperature resistance of aluminum-matrix composites using an acid phosphate binder. Part I. Binders, *J. Mater. Sci.* 28 (6) (1993) 1435–1446.
- [2] W.D. Kingery, Fundamental study of phosphate bonding in refractories. I. Literature review, *J. Am. Ceram. Soc.* 33 (1950) 239–241.
- [3] J.E. Cassidy, Phosphate bonding then and now, *Am. Ceram. Soc. Bull.* 56 (7) (1977) 640–643.
- [4] W.D. Kingery, Fundamental study of phosphate bonding in refractories. II. Cold-setting properties, *J. Am. Ceram. Soc.* 33 (1950) 242–247.
- [5] Y.A. Pirogov, L.N. Soloshenko, N.M. Kvasman, Mullite-corundum ramming mass containing graphite and silicon carbide additives, *Refractories* 28 (3/4) (1987) 117–119.
- [6] J.D. Birchall, N.M. Alford, K. Kendall, Effect of chemical bonding at low temperature on the mechanical properties of an unsintered SiC compact, *J. Mater. Sci. Lett.* 6 (12) (1987) 1456–1458.
- [7] C. Toy, O.J. Whittemore, Phosphate bonding with several calcined aluminas, *Ceram. Int.* 15 (3) (1989) 167–171.
- [8] W.H. Gitzen, L.D. Hart, G. Maczura, Phosphate-bonded alumina castables: some properties and applications, *Ceram. Bull.* 35 (1956) 217–223.
- [9] J.A. Fernando, D.D.L. Chung, Improving an alumina fiber filter membrane for hot gas filtration using an acid phosphate binder, *J. Mater. Sci.* 36 (21) (2001) 5079–5085.
- [10] J.A. Fernando, D.D.L. Chung, Pore structure and permeability of an alumina fiber filter membrane for hot gas filtration, *J. Porous Mater.* 9 (3) (2002) 211–219.
- [11] D.D.L. Chung, Phosphate binder for fabricating preforms for making metal-matrix composites by liquid metal infiltration, U.S. Patent 5,536,686.
- [12] C.A. Martin, I.G. Talmy, High temperature mechanical properties of phosphate-bonded ceramics, *Ceram. Eng. Sci. Proc.* 16 (4) (1995) 587–594.
- [13] J.C. Knight, T.F. Page, Mechanical properties of highly porous ceramics—part II: slow crack growth and creep, *Br. Ceram. Trans.* 85 (2) (1986) 66–75.
- [14] V. Jokanovic, G. Djurkovic, R. Curcic, Creep and microstructure in refractory materials, *Am. Ceram. Soc. Bull.* 77 (7) (1998) 61–65.
- [15] S.C. Mitchell, Hot gas particulate filtration, IEA Coal Research, London, 1997.
- [16] W. Kingery, H. Bowen, D. Uhlmann, *Introduction to Ceramics*, John Wiley, New York, 1975.
- [17] B.S. Bobrov, I.G. Zhigun, L.V. Kiseleva, A.N. Abyzov, L.A. Kir'Yanova, Phase composition of binder based on aluminophosphate cementing agent and changes in it on heating, *J. Appl. Chem. USSR* 59 (12(pt. 1)) (1986) 2424–2428.
- [18] C.T. Chia, K.A. Khor, Y.W. Gu, Dynamic mechanical properties of  $\text{ZrO}_2/\text{NiCoCrAl}_y$  composite coatings, *Thin Solid Films* 358 (1) (2000) 139–145.
- [19] J. Zhang, R.J. Perez, E.J. Lavernia, Dislocation-induced damping in metal matrix composites, *J. Mater. Sci.* 28 (3) (1993) 835–846.
- [20] X. Fu, D.D.L. Chung, Effect of admixtures on the thermal and thermo-mechanical behavior of cement paste, *ACI Mater. J.* 96 (4) (1999) 455–461.
- [21] J.R. Olson, Thermal conductivity of fibrous insulating materials, *Am. Ceram. Soc. Bull.* 76 (3) (1997) 81–84.